Photoconductivity Studies of Defects in p-Type Silicon: Boron Interstitial and Aluminum Interstitial Defects*

M. CHERKI† AND A. H. KALMA‡

Groupe de Physique des Solides, de l'Ecole Normale Supérieure,§ Faculté des Sciences de Paris, France

(Received 19 March 1969; revised manuscript received 25 August 1969)

Two defects introduced in p-type silicon by 1.5-MeV electron irradiation are studied by means of infrared photoconductivity, including the measurement of the stress-induced dichroism. They are identified as being dopant atoms in interstitial positions produced by the silicon interstitial-impurity atom replacement mechanism proposed by Watkins. They are introduced by room-temperature irradiations as well as by irradiations performed at 77, 20.4, and 4.2°K. They disappear during annealing at temperatures ~250–300°C. The symmetry of these defects C_{3v} is deduced from the low-temperature stress-induced dichroism of the photoconductivity which is associated with electronic reorientation among different configurations. This C_{3v} symmetry can be explained by distortion of a possible Jahn-Teller type of a configuration in which the dopant atom was originally in a tetrahedral position. The defect response to the stress is determined by the value of the term in the piezospectroscopic defect tensor which characterizes the relative change in defect energy per unit strain. This value is $\simeq -12$ eV/(unit strain). Numerical values of the dichroic ratios show that the photoconductivity transition which is observed corresponds to a distribution of dipole moments which is an ellipsoid of rotation about the trigonal axis of the defect. They also allow the determination of this distribution.

I. INTRODUCTION

IN studies of defects in silicon, little information is available concerning interstitial defects. This is in contrast to the knowledge available concerning vacancy defects, where the vacancy itself has been studied extensively,[1] and the fate of mobile vacancies, which form vacancy-defect complexes, has been largely resolved[2–4] However, recent experiments[2–4] have shed some light on interstitial defects, though the silicon interstitial has not been positively identified.

Electron paramagnetic resonance work by Watkins[2–4] has provided much of the current knowledge concerning interstitial defects. From these studies it appears that the silicon interstitial is mobile in p-type silicon at temperatures as low as 4.2°K. This mobile interstitial changes places with a substitutional acceptor atom, the result being that the observed defect is an interstitial dopant atom. The aluminum interstitial, the most completely studied of these interstitial defects, can be produced at temperatures at least as high as 300°K. The production rate varies in a complicated manner with temperature, being comparable at 20.4 and 300°K but much lower at ~100°K. The equilibrium charge state of the defect when observed at 20.4°K with the Fermi level locked to the substitutional acceptor level at $E_v+(0.05$ eV) is doubly positive. In this charge state, the defect has the full T_d symmetry.[5] Illumination with band-gap light or a burst of radiation at low temperature can reduce the Al_i^{++} concentration by at least a factor[6] of 2 indicating that another charge state of the defect can exist under these conditions. The dopant interstitials are stable up to temperatures of ~250°C. The supposed low-temperature mobility of the silicon interstitial in p-type material and its trapping by dopant atoms means that the dopant impurity will affect the nature of the defects formed even at irradiation temperatures as low as 4.2°K.

Vacancy motion, however, does not occur until higher temperatures. In p-type silicon, the vacancy (in its neutral charge state) has been shown to be immobile below ~150°K.[2–4] It is possible that a mobile vacancy in another charge state can exist under irradiation; however, in n-type silicon the doubly negative vacancy is immobile below ~60°K.[2–4] Also, although there have been effects attributed to vacancy motion under irradiation at temperatures as low as 20°K[7] in n-type silicon and ~60°K in p-type silicon,[7] only the motion of interstitials has been reported thus far below ~60°K in p-type materials. Thus, any low-temperature damage (<50°K) in p-type silicon involving nonintrinsic defects should be dominated principally by interstitial effects.

Infrared photoconductivity can be a valuable probe in studying defects formed at low temperatures, as it is not necessary to heat the sample to obtain various properties of the defects, including energy-level posi-

* This work has been supported by the Delegation Generale à la Recherche Scientifique et Technique and the U. S. Air Force (Cambridge Air Force Laboratories).

† This work is part of the thesis being prepared by M. Cherki for the degree of Docteur es Sciences at the Université de Paris.

‡ Present address: Gulf General Atomic, San Diego, Calif.

§ Laboratoire associé au Centre National de la Recherche Scientifique.

[1] G. D. Watkins, J. Phys. Soc. Japan 18, Suppl. II, 22 (1963).

[2] G. D. Watkins, *Radiation Effects in Semiconductors* (Plenum Press, Inc., New York, 1968), p. 67.

[3] G. D. Watkins, in *Radiation Damage in Semiconductors* (Dunod Cie., Paris, 1965), p. 97.

[4] G. D. Watkins, in *Symposium on Radiation Effects in Semiconductor Components* (Journées d'Electronique, Toulouse, France, 1968), p. A1-0.

[5] The nomenclature we use to denote groups and representations follows that used in M. Hamermesh [*Group Theory* (Addison-Wesley Publishing Co., Inc., Reading, Mass., 1964)] with the exception that the triplet notation is changed from F to T.

[6] G. D. Watkins (private communications).

[7] K. Matsui and P. Baruch, *Lattice Defects in Semiconductors* (Pennsylvania State University Press, University Park, Pa., 1968), p. 282.

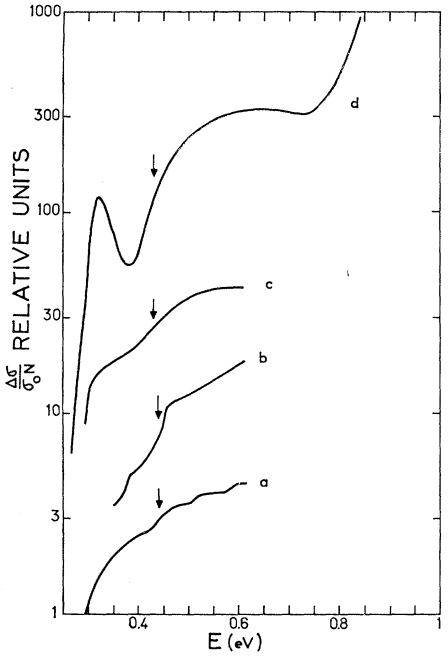

FIG. 1. Introduction of the D_i defects in boron-doped silicon by 1.5-MeV electrons at different irradiation temperatures: (a) $T_{irr}=4.2$°K, fluence $=1.25\times10^{16}$ e/cm²; (b) $T_{irr}=20.4$°K, fluence $=7\times10^{16}$ e/cm²; (c) $T_{irr}=77$°K, fluence $=1.2\times10^{17}$ e/cm²; (d) $T_{irr}=300$°K, fluence $=5\times10^{17}$ e/cm². The relative positions of the spectra are arbitrary for convenient display.

tions. Used in conjunction with the application of uniaxial stress, this technique also provides information about the microscopic configurations of defects, since stress preferentially aligns the defects and this alignment results in a measurable anisotropy of the photoconductivity spectra.[8,9]

In photoconductivity studies of irradiated p-type silicon, one of the dominant energy levels found arises at $\sim E_v+0.4$ eV.[7–10] Vavilov *et al.*[10] found the production of this level depended on the acceptor concentration and deduced that it involved the acceptors. Matsui and Baruch[7] found that the level could be produced by irradiation at 20.4°K in material doped with boron, gallium, or aluminum and concluded that the silicon interstitial was involved in the production. They also supposed that the defect involved was a boron atom in an interstitial position, owing to residual boron in material doped with other acceptors.

In an article in which the major topic was the study of the divacancy, Cheng[9] reported results obtained with the application of uniaxial stress concerning this level in boron-doped material. From the fact that there was no dichroism appearing in the photoconductivity spectrum for a [100] stress, he deduced that the symmetry of the defect involved was a ⟨111⟩ symmetry. We have expanded Cheng's stress studies of this energy level in boron-doped and aluminum-doped silicon and will present data that leads to the conclusion that the defect giving rise to the level is the dopant atom in an interstitial position. We shall also present a model of the configuration of the defect which agrees with results obtained by uniaxial stress experiments.

II. EXPERIMENTAL PROCEDURE

Bridge samples were cut from commercially available boron-doped or aluminum-doped silicon ingots (obtained from S.I.L.E.C.[10a]) containing $\sim10^{18}$ oxygen atoms/cc (pulled crystals) as the influence of oxygen content on the defects studied was found to be negligible[7,10,11] and pulled crystals were more readily available. The sample resistivities at room temperature were nominally 1 Ω cm before irradiation. An optical polish of the sample surfaces exposed to the infrared beam followed by a chemical etch was used to achieve good transmission. Contacts were made by evaporating aluminum on the sample arms and attaching 0.15-mm-diam gold wires by thermal compression using a local heating technique.[12] Crystal orientations were determined by x-ray diffraction.

The cryostat used was a conduction-cooling, liquid-helium type with a central tube for the coolant gas condensate. The tail piece was designed so that stress could be applied to the sample *in situ* with a mechanism utilizing oil pressure applied by a screw-operated piston. This mechanism was used with stresses up to ~3500 kg/cm².

The irradiations were performed with a 3.0-MeV Van de Graaff electron accelerator at liquid-helium, liquid-hydrogen, liquid-nitrogen, and room temperatures with the sample in the cryostat in all cases. The beam current was adjusted so that the sample temperature rise was <1°C at liquid-helium and -hydrogen temperatures ($I<0.1$ μA) and <15°C at liquid-nitrogen and room temperatures ($I<10$ μA).

The photoconductivity spectra were measured at liquid-nitrogen temperature or the irradiation temperature if the latter was lower. The measurements were performed with two Princeton Applied Research (PAR) model HR8 lock-in amplifiers equiped with type A high-impedance preamplifiers. They were used to measure simultaneously both the sample signal and beam intensity (using a thermocouple intercepting a portion of the beam). The signals were fed into a PAR model RC10 ratiometer to obtain the normalized photoconductivity signal.[13] The sample channel utilized a

[8] A. H. Kalma and J. C. Corelli, Phys. Rev. **173**, 734 (1968).
[9] L. J. Cheng, *Radiation Effects in Semiconductors* (Plenum Press, Inc., New York, 1968), p. 143.
[10] V. S. Vavilov, A. F. Plotnikov and V. D. Tkachev, Fiz. Tverd. Tela. 4, 3446 (1962) [English transl.: Soviet Phys.—Solid State 4, 2522 (1963)].
[10a] La Société Industrielle de Liaisons Electriques, France.
[11] K. Matsui, Ph.D. thesis, Université de Paris, 1965 (unpublished).
[12] E. Matsuura, K. Matsui, and R. R. Hasiguti, J. Appl. Phys. **33**, 1610 (1962).
[13] This gives the photoconductivity per unit incident energy. In drawing the figures, we have multiplied by the quantum energy and plot the photoconductivity per incident photon.

Keithley model 603 electrometer and the thermocouple channel, PAR models CR4 and AM1 preamplifiers for impedance matching. A CODERG evacuable grating monochromator equipped with the appropriate gratings and filters was used as the source of monochromatic light. The light source was a globar. The numerical aperture of the spectrometer was $f/5$ and the resolution used was $\lesssim 0.05$ μ. A wire grid polarizer (PERKIN–ELMER 186-0240), the efficiency of which was better than 98%, was placed in the monochromatic beam to polarize the infrared light. Simultaneous measurement of light intensity and photoconductivity signal eliminated difficulties arising from the polarization of the light by gratings.

Illumination with monochromatic light resulted in voltage changes across the samples which ranged from $\Delta V/V \sim 10^{-7}$ to $\sim 5\times 10^{-4}$. The photoconductivity single as a function of monochromatic light intensities was linear in the range of intensities which were employed. The extrinsic signal had the same sign as the intrinsic one except in one particular type of experiment (irradiation at nitrogen temperature—simultaneous illumination of the sample by monochromatic and white light). The effect of stray light was negligible. Illumination by white light was performed with a flashlight bulb powered by a 6-V battery.

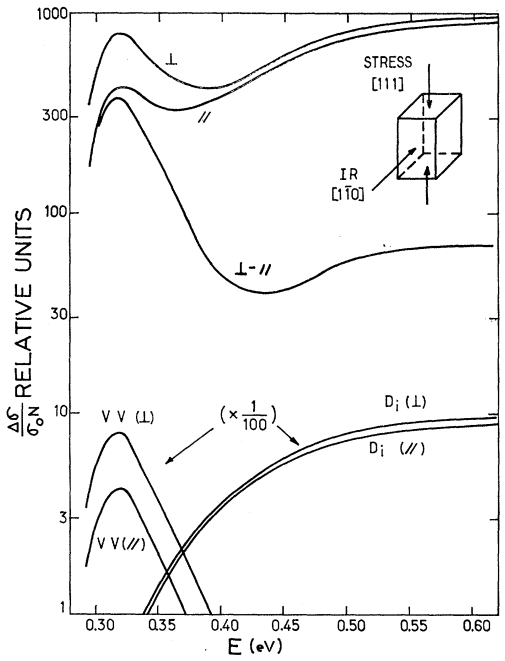

FIG. 2. Determination of the shape of the transition arising from the D_i defect: aluminum-doped silicon irradiated at 77°K with 4×10^{17} e/cm² of 1.5 MeV. Photoconductivity spectra at 77°K after room-temperature annealing. Stress of 2240 kg/cm².

III. DEFECT IDENTIFICATION

A. Influence of Dopant on Photoconductivity Spectrum

The photoconductivity spectrum measured at nitrogen temperature of p-type silicon irradiated at room temperature has typically the shape which is shown in Fig. 1(d). The main features of this spectrum are a photoconductivity "band" with a maximum at 0.32 eV and an important rise of the photoconductivity in the region of ~0.4 eV. The band has been associated with the divacancy by Cheng[9] and its shape explained as being due to a transition between two levels of the divacancy, the lower one in equilibrium with the valence band. The rise of the photoconductivity in the region of ~0.4 eV is the object of our study. We will label as D_i defects the defects which are associated with this photoconductivity increase.

Photoconductivity being an additive process, the total amount of photoconductivity in the region from 0.3 eV to higher energies can arise from D_i defects as well as from other defects. It is then necessary to determine the exact shape of the hole transition from the D_i defect level to the valence band, if we want to study the effect of dopant atoms on this transition. This can be accomplished with uniaxial stress experiments; application of stress to the sample at 80°K results in a dichroism[14] of the photoconductivity spectra which can be attributed to electronic reorientation of the defects. As has been previously shown,[8] dichroism measurements provide a way of determining unambiguously the shape of a transition.

The determination of the shape of the transition associated with D_i defects is presented in Figs 2 and 3 for aluminum- and boron-doped samples, respectively. The spectra labelled ⊥ and ‖ are the photoconductivity spectra of the samples under stress performed with light polarized perpendicular and parallel to the stress direction.

D_i defects start ionizing in an energy region of ~0.350 eV. Thus, the total photoconductivity $\mathcal{P}$ for a photon energy greater than 0.350 eV can be considered as the sum of a photoconductivity which corresponds to the ionization of the D_i defects ($\mathcal{P}_{D_i}$) and of a possible background photoconductivity associated to other defects in the crystal ($\mathcal{P}_{\text{bkg}}$). When the light is polarized parallel to the stress, we write for photon energies greater than 0.350 eV

$$\mathcal{P}_{\parallel}(E)=\mathcal{P}_{\parallel D_i}(E)+\mathcal{P}_{\parallel \text{bkg}}(E). \quad (1)$$

When the light is polarized perpendicular to the stress, we write

$$\mathcal{P}_{\perp}(E)=\mathcal{P}_{\perp D_i}(E)+\mathcal{P}_{\perp \text{bkg}}(E). \quad (2)$$

If the D_i defect gives rise to a dichroism and if we assume that this dichroism only arises from a difference in the populations of the different configurations of the defect, then the shape of the transition will be the same for both polarizations and the dichroism of the

[14] By "dichroism" we mean the ratio of the photoconductivity due to the single level in question measured with the light polarized perpendicular to the stress direction to that with the light polarized parallel to the stress direction.

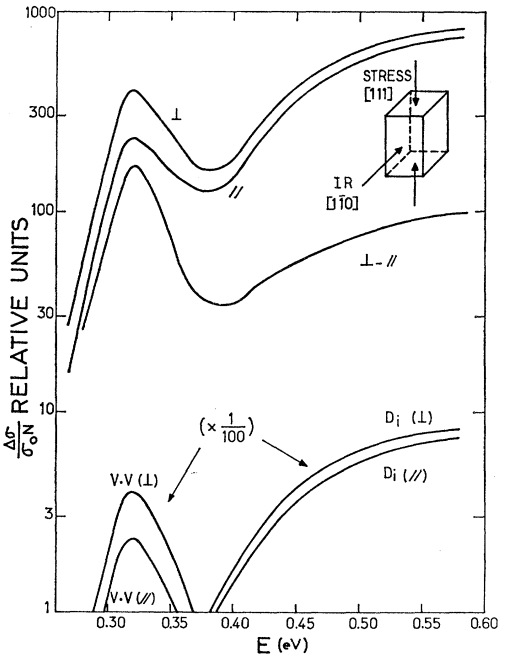

FIG. 3. Determination of the shape of the transition arising from the D_i defect: boron-doped silicon irradiated at 300°K with 5×10^{17} e/cm² of 1.5 MeV. Photoconductivity spectra at 77°K. Stress of 1700 kg/cm².

transition will be the same for all photon energies. Now, if D is the dichroic ratio corresponding to the D_i defect transition,

$$D=\frac{\mathcal{P}_{\perp D_i}(E)}{\mathcal{P}_{\parallel D_i}(E)}=\frac{\mathcal{P}_{\perp}(E)-\mathcal{P}_{\perp\mathrm{bkg}}(E)}{\mathcal{P}_{\parallel}(E)-\mathcal{P}_{\parallel\mathrm{bkg}}(E)}. \tag{3}$$

In our case, the photoconductivity step being great for $E\gtrsim0.45$ eV, $\mathcal{P}_{\mathrm{bkg}}$ must be small, and it is reasonable to assume that[15]

$$\mathcal{P}_{\perp\mathrm{bkg}}(E)=\mathcal{P}_{\parallel\mathrm{bkg}}(E). \tag{4}$$

Then

$$\mathcal{P}_{\perp}(E)-\mathcal{P}_{\parallel}(E)=\mathcal{P}_{\perp D_i}(E)-\mathcal{P}_{\parallel D_i}(E)=\left(\frac{D-1}{D}\right)\mathcal{P}_{\perp D_i}(E), \tag{5}$$

and the difference $\mathcal{P}_{\perp}(E)-\mathcal{P}_{\parallel}(E)$ (labelled ⊥-∥ in Figs. 2 and 3) gives the exact shape of the transition from ~0.45 eV to higher energies (This shape labelled D_i is shown at the bottom of Figs. 2 and 3.)

Since we observe that for $E>0.45$ eV

$$\mathcal{P}_{\perp}(E)=k(\mathcal{P}_{\perp}-\mathcal{P}_{\parallel})=k\left(\frac{D-1}{D}\right)\mathcal{P}_{\perp D_i}(E), \tag{6}$$

where k is a constant, we find that the background photoconductivity for $E>0.45$ eV is ~0, which shows that the assumption of Eq. (4) was reasonable.

[15] This is useful mathematically but not necessary in practice.

The same procedure is applied to the photoconductivity band of the divacancy. The background (essentially due to the D_i defects) is found to be zero for $E\lesssim0.30$ eV in aluminum-doped sampled and $E\lesssim0.35$ eV in boron-doped samples. The shape of the transition corresponding to the divacancy and labelled VV at the bottom of Figs. 2 and 3 is determined again by the spectrum ⊥-∥.

In the region from $\simeq E_v+0.30$ eV in aluminum-doped samples, and $\simeq E_v+0.35$ eV in boron-doped samples, to $E_v+0.45$ eV,

$$\mathcal{P}_{\perp}(E)=\mathcal{P}_{\perp D_i}(E)+\mathcal{P}_{\perp\mathrm{VV}}(E) \tag{7}$$

and

$$\mathcal{P}_{\parallel}(E)=\mathcal{P}_{\parallel D_i}(E)+\mathcal{P}_{\parallel\mathrm{VV}}(E), \tag{8}$$

where $\mathcal{P}_{\perp D_i}(E)$ and $\mathcal{P}_{\perp\mathrm{VV}}(E)$ are the contributions of D_i defects and the divacancies, respectively. These contributions are comparable, and the divacancy band with its dichroism must be extrapolated and then substracted from the spectrum in order to get the shape of the transition corresponding to D_i defects. This introduces an uncertainty in determining the leading edge of the transition corresponding to D_i defects that we evaluate to 0.010 eV for boron-doped samples and 0.015 eV for aluminum-doped samples. The leading edge of the transition is then located for boron-doped samples at $E_v+0.330\pm0.010$ eV and for aluminum-doped samples at $E_v+0.290\pm0.015$ eV. Because of the errors on the leading edge, we have preferred to choose another point to characterize the energy position of the transition; we have arbitrarily chosen the point where 33% of the maximum number of carriers are excited out of the D_i defects.[16] (It is the point nearest to the onset of the ionization where the divacancy is nearly negligible.)

In these conditions, the position of the energy level associated with the D_i defects is $E_v+0.395$ eV in aluminum-doped samples and $E_v+0.430$ eV in boron-doped samples. We estimate that the error in the determination is ±0.005 eV for boron-doped samples and ±0.010 eV for aluminum-doped samples. The latter is larger due to the greater effect of the divacancy at the lower energy. These errors are sufficient to encompass variations observed in samples doped with the same element. The resolution of the spectrometer in this energy region is approximately 0.005 eV.

The level position is independent of irradiation dose in samples with the same dopant if the measurement is carried out at the same temperature.[17] When the measurements were carried out at 20°K (and even more so at 4°K) uniaxial stress experiments did not allow the determination of the energy-level position with enough precision but showed that the defect involved was the

[16] We shall label this value the energy-level position, since there is no theoretical method to determine the exact position from the shape of the spectrum.

[17] With liquid-nitrogen temperature measurements and above, the level position does not change from 77 to at least 125°K.

same. We, therefore, characterized this position again by the point where we estimate that 33% of the maximum number of carriers are excited out of the D_i defects. Evaluation of the background photoconductivity was made by extrapolating the rest of the spectrum in the region where D_i defects ionize.

The difference in the position of the energy levels arising from the D_i defects as measured at 77°K in aluminum-doped samples and boron-doped samples is shown Fig. 4. This difference in energy-level position with different dopants leads to the conclusion that the dopant atoms are involved in the D_i defects.

Energy levels in p-type silicon at the same general position have been reported to arise in boron-doped[7–9] and indium-doped[8] floating-zone (low oxygen content) crystals and gallium-doped[7] pulled crystals. It thus appears that similar D_i defects are formed in p-type silicon crystals doped with any group-III acceptor and that oxygen is not necessary for this formation.

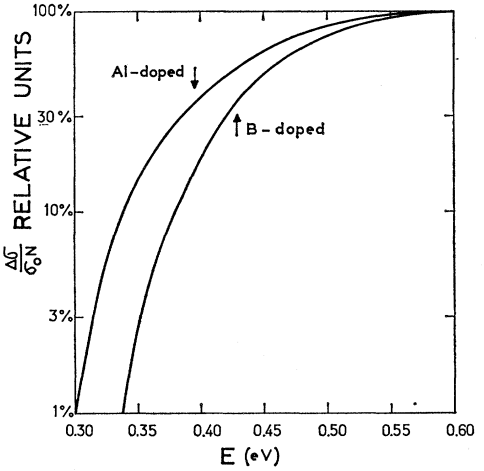

FIG. 4. Comparison of the shapes of the transitions arising from the D_i defects in aluminum-doped and boron-doped silicon as determined in Figs. 2 and 3. The curves are normalized to 100% at a high enough energy (0.6 eV) that the photoconductivity is no longer increasing.

B. Influence of Irradiation Temperature

Since vacancies and interstitials in silicon become mobile at different temperatures,[2–4] studies in which defects are produced at different temperatures give information as to whether vacancies or interstitials are involved in specific defects. We have found that the D_i defects are produced by 4.2, 20.4, 77, and 300°K electron irradiations. Figure 1 shows the photoconductivity spectra obtained for boron-doped silicon following 1.5-MeV electron bombardment at these temperatures.

The position of the energy level (indicated by the arrows) introduced by 77 and 300°K electron irradiations is determined by stress measurements at 77°K, as has been previously described. Dichroism measurements were performed also at 20°K with the boron-doped samples; at these temperatures, the levels observed are sharper and slightly displaced toward higher energies. Experimental limitations did not allow heavy irradiations at 20°K, which would have resulted in too high a sample resistance. Therefore, the signal-to-noise ratio did not permit a precise numerical determination of dichroic ratios. However, their sense and relative magnitude were the same as measured with the stress applied at 77°K showing that the defects involved are the same.

Similar results to those shown in Fig. 1 have been obtained for aluminum-doped silicon. Although there have been effects attributed to vacancy motion under irradiation at temperatures as low as 20°K,[7,11] it is unlikely that many vacancies were mobile during the 20.4 and 77°K irradiations of the samples shown in Fig. 1, as there were nearly no divacancies present immediately after irradiation. The presence of divacancies was monitored by the 0.32-eV photoconductivity band[9] which was absent in the spectra measured at 4.2, 20.4, and 77°K immediately after irradiation while it appeared in the spectra measured at these temperatures after annealing at room temperature. The increase in number of divacancies was presumably effected by vacancy motion and pairing. During the room-temperature annealing, the number of D_i defects was essentially unaffected. The absence of the divacancy band was not always observed and the divacancy appeared to be directly produced under 77°K irradiation in one aluminum-doped sample.[18] However, the D_i defects were always produced at all temperatures. Since the D_i defects are produced without apparent vacancy motion at 4.2, 20.4, and 77°K, we conclude either that the D_i defects are produced directly or that the silicon interstitial is involved in the production process. Since the dopant atoms are involved in the D_i defects, and since it is highly improbable that the dopant atoms are involved in a direct production process, we conclude that the D_i defects are created by an impurity-silicon interstitial-interaction mechanism. In light of the evidence presented by Watkins[2–4] that silicon interstitials produced by irradiation migrate to substitutional acceptors and interchange with them resulting in dopant atoms in interstitial sites, we conclude that *the D_i defects are*, in fact, *dopant interstitial atoms*.

In samples irradiated at 77°K, a level at $E_v+0.35$ eV not normally observed could be seen in the photoconductivity spectrum during the illumination of the samples with white light (Fig. 5). The photosensitivity, which was lower after irradiation, was increased by the white light and also increased upon annealing to higher temperatures even though the resistance decreased. This behavior persisted to above 300°C. We do not

[18] For irradiations nominally performed at 77°K, the temperature was not well controlled and may have been ~10°C different between two experiments.

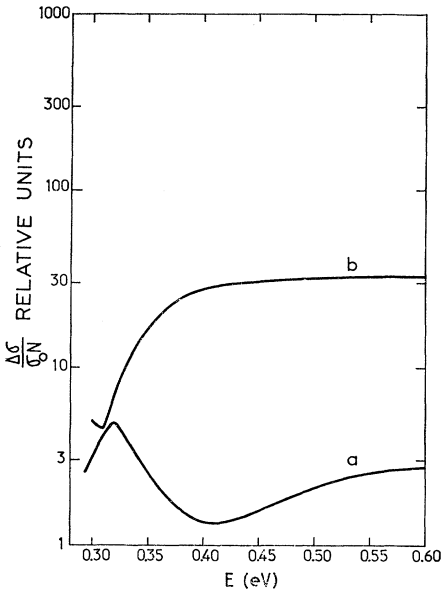

FIG. 5. Influence of white light on boron-doped silicon irradiated with 1.5-MeV electrons at 77°K: (a) no white light; (b) with white light. The ordinate is proportional to the relative change in resistivity per photon, and the relative position of the spectra is correct.

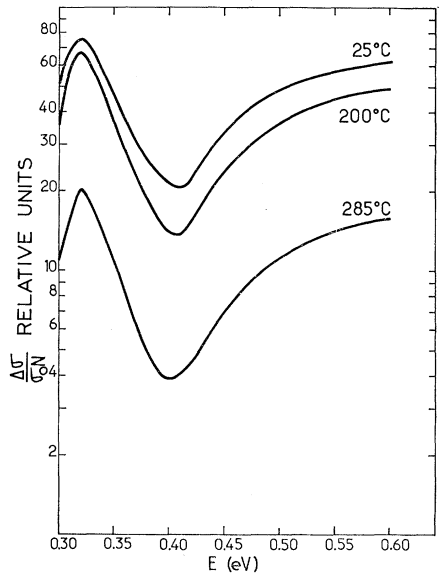

FIG. 7. Isochronal annealing (10 min at each temperature) of boron-doped silicon irradiated at 300°K with 2.65×10^{17} e/cm² of 1.5 MeV. The spectra are labelled with the annealing temperature and they were measured at 77°K. The ordinate is proportional to the relative change in resistivity per photon and the relative positions of the spectra are correct with the exception that the 25°C spectrum has been displaced one-tenth of a decade toward the top for clarity.

know the nature of the defect giving rise to this new level at present. It might be the same as one giving rise to an energy level in the same position that is produced at 4.2°K by 1.5-MeV electrons (Fig. 1). We observed similar behavior in a sample irradiated at room temperature by 0.9-MeV electrons but not by 1.5-MeV electrons, so the production process of this defect is unclear.

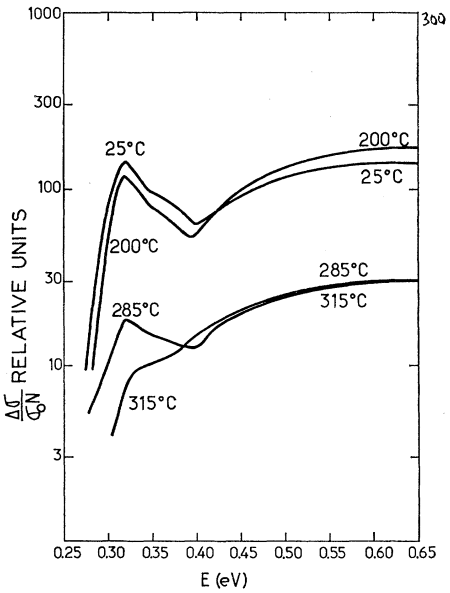

FIG. 6. Isochronal annealing (15 min at each temperature) of aluminum-doped silicon irradiated at 300°K with 2×10^{17} e/cm² of 1.5 MeV. The spectra are labelled with the annealing temperature and they were measured at 77°K. The ordinate is proportional to the relative change in resistivity per photon and the relative positions of the spectra are correct.

C. Damage Recovery

The D_i defects disappear in the temperature range of ~250–300°C. Figures 6 and 7 show the effects of isochronal annealing on the photoconductivity spectra of an aluminum-doped and a boron-doped sample, respectively, irradiated at room temperature. Figures 8 and 9 show the relative concentration of the divacancy (as measured by the 0.32-eV peak[9]) and the relative concentration of the D_i defects (as measured by the maximum photoconductivity of the associated transition) as a function of the annealing temperature.[19] The annealing stage at ~250–300°C is clearly evident here. This temperature region is the same as the region where Watkins[3,4] observed the aluminum interstitials to anneal. This is another argument for identifying the D_i defects with dopant interstitial atoms.

The process by which the D_i defects disappear in this temperature region is unclear. It is apparent that in the sample doped with aluminum (Fig. 8) some of the D_i defects were stable above 300°C. This was not the case

[19] Spectra of Fig. 6 and Fig. 7 have the normal shape of a 77°K photoconductivity spectrum of a room-temperature irradiated sample; extraction of the D_i defect and divacancy components is thus made as explained in Sec. III A. In Figs. 8 and 9 concentrations of the two defects can not be compared absolutely to each other with this measurement.

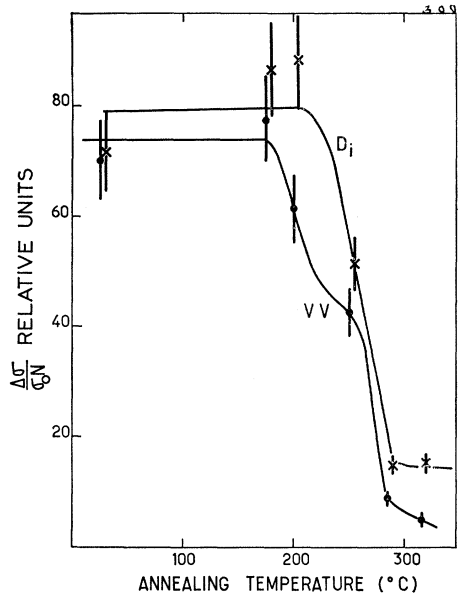

FIG. 8. Comparison of the isochronal annealing behavior of the D_i defects and the divacancy. The data shown are for the aluminum-doped sample whose spectra are presented in Fig. 6. The points for the D_i defects are shifted 5°C on the abscissa for clarity.

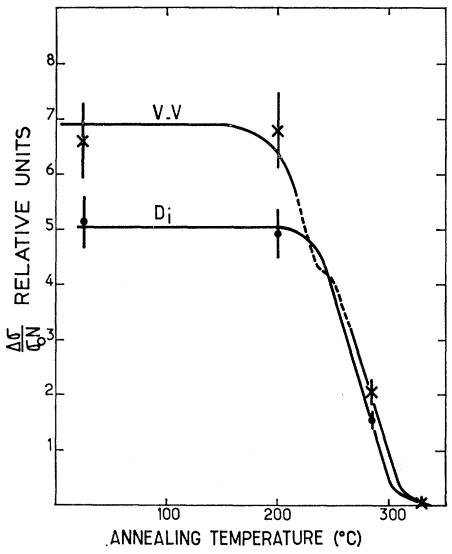

FIG. 9. Comparison of the isochronal annealing behavior of the D_i defects and the divacancy. The data are for the boron-doped sample whose spectra are presented in Fig. 7.

for any of the boron-doped samples studied, where the annealing was apparently complete in this stage. This difference in annealing behavior could be caused by the different dopants or by a process in which the D_i defects disappear by the trapping of other mobile defects, e.g., the aluminum-vacancy pair[20] and the divacancy[21] (whose annealing in this temperature region appears clearly in Figs. 8 and 9). Certain other results[3,11,22,23] suggest the second process and that the D_i defects might not undergo long-range migration until ~1000°C; however, insufficient information is available to warrant further speculation.

Regardless of the annealing mechanism involved in the damage recovery at 250–300°C, the disappearance of the D_i defects in this temperature region together with their introduction at low temperatures and dependence on the dopant strongly favor their identification as dopant atoms in interstitial positions.

IV. MICROSCOPIC CONFIGURATION OF D_i DEFECTS

A. Symmetry of D_i Defects

In order to interpret more readily the experimental stress results, it will be convenient at this point to present a description of the configuration of the D_i defect which has been used to calculate the dichroic ratios. In the silicon lattice, there are as many empty tetrahedral positions as occupied lattice sites. We assume that the dopant atom occupies one of these positions. This configuration is shown in Fig. 10. The interstitial atom, labelled I, is in the tetrahedral site surrounded by four-nearest-neighbor silicon-lattice atoms, labelled a, b, c, and d, in the same manner as a substitutional atom.

This configuration with the full T_d symmetry is that of the aluminum interstitial in its doubly positive charge state observed by Watkins[6] in EPR experiments. Since such a symmetry would result in a defect insensitive to stress, we deduce from the observation of dichroism in the photoconductivity experiments that D_i defects do not have the full T_d symmetry and thus are not in a doubly positive charge state. In a different charge state, the defect may undergo a Jahn-Teller

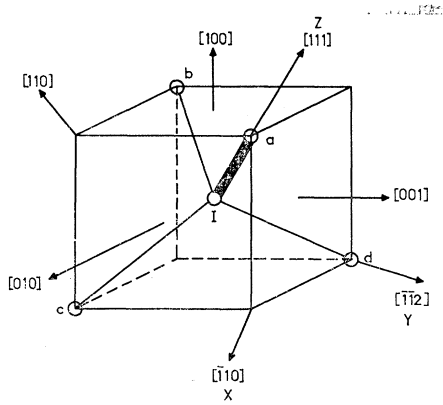

FIG. 10. Configuration of the D_i defects.

[20] G. D. Watkins, Phys. Rev. **155**, 802 (1967).
[21] G. D. Watkins and J. W. Corbett, Phys. Rev. **138**, A555 (1965).
[22] J. W. Mayer and O. J. Marsh, in *Applied Solid State Science*, edited by C. J. Kriessman and R. Wolfe (Academic Press Inc., New York, 1968), Chap. IV & V. This review contains the references to the original experiments.
[23] N. G. Blamires, M. D. Matthews, and R. S. Nelson, Phys. Letters **28A**, 178 (1968).

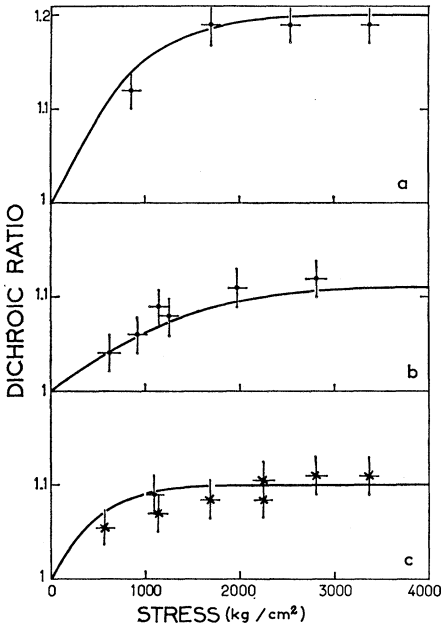

FIG. 11. Dichroism versus stress. (a) stress=[110], IR=[001]; (b) stress=[110], IR=[1$\bar{1}$0]; (c) stress=[111], IR=[1$\bar{1}$0]. The crosses are for aluminum-doped silicon and the dots for boron-doped silicon.

distortion[24] from the T_d symmetry; the possible distortions are to a D_{2d} symmetry (that of the vacancy V^+) or to a C_{3v} symmetry. D_{2d} is inconsistent with the fact that there is a dichroism observed for a ⟨111⟩ stress. On the other hand, a C_{3v} symmetry is not only consistent with a ⟨111⟩ stress-induced dichroism, but also with the observed lack of dichroism for a ⟨100⟩ stress. Furthermore, using the C_{3v} configuration of the interstitial as the basis for theoretically calculating the dichroic ratios results in very good agreement with the experimentally observed ratios. We consider this the strongest justification for the configuration described above since other possible models fail; for instance, the model proposed by Watkins[25] for the defect he tentatively interpreted as the boron interstitial does not account for the observed values of the dichroic ratios. The C_{3v} configuration of the defect has been depicted in Fig. 10. Three of the nearest-neighbor silicon atoms remain equivalent and the fourth atom (labelled *a* in Fig. 10) becomes nonequivalent to them. The *z* axis of the configuration is then the [111] axes containing the nonequivalent silicon atom. There are thus four possible configurations of the defect corresponding to the four [111] axes allowable for the *z* axis of the defect. We shall label each configuration by the letter corresponding to the silicon atom which is along the *z* axis. Therefore, the configuration depicted in Fig. 10 is labelled *a*.

Let us now examine the type of the photoconductivity transition which is expected for this defect. The probability of transition will be proportional to the matrix element for an electric dipole transition[26] $\langle\phi_0\psi_i|\mathbf{r}|\psi_f\rangle$, where ϕ_0, ψ_i, and ψ_f are the one-electron wave function corresponding to the top of the valence band ($\mathbf{k}=0$), the *n*-electron wave function corresponding to the initial state of the defect, and the $(n+1)$-electron wave function corresponding to the final state of the defect. (We will discuss the charge state of the defect in Sec. IV C.)

The allowed dipole moments of the transition are the ones which transform as the representations contained in the product of the representations of initial and final states. For a T_d configuration of the interstitial, the valence band edge states which transform as Γ_{25}' in the O_h space group of the silicon lattice will be resolved into T_2 states in T_d. (We are not considering the spin-orbit interaction which is of the order of 0.04 eV.) For a C_{3v} distortion of the defect these T_2 states in T_d will be resolved into A_1+E states in the C_{3v} group. We will label Γ_i and Γ_f the representations of ψ_i and ψ_f (which must be equal to one of the representations of the C_{3v} group, i.e., A_1, A_2, or E). The allowed dipole moments transform as the representations contained in $(A_1+E)\times\Gamma_i\times\Gamma_f$. In C_{3v}, a *z*-type electric dipole transforms as A_1 and an *xy*-type electric dipole transforms as E. If the product $(A_1+E)\times\Gamma_i\times\Gamma_f$ contains only E, it will be an *xy*-type dipole, if it contains the sum (A_1+E), all directions of dipole moments will be allowed and we will observe a transition with a "volume oscillator", this volume being an ellipsoid of rotation about the axis of the center. If we assume that the dipole moment is a *z*-type or an *xy*-type dipole, the calculated dichroic ratios turn out to be at least two times greater than the experimental ones. On the other hand, the hypothesis of a volume oscillator appears better substantiated, since we will show that this leads

TABLE I. Dichroic ratios at saturation for different stress directions.

Sample dopant	Stress direction	Infrared direction	Dichroism (measured at saturation)
B	[100]	[010]	1
B	[110]	[001]	1.19
B[a]	[110][a]	[001][a]	1.17[a]
B	[110]	[1$\bar{1}$0]	1.12
B[a]	[111][a]	[1$\bar{1}$0][a]	1.10[a]
B[a]	[100][a]	[011][a]	1[a]
Al	[111]	[1$\bar{1}$0]	1.11

[a] After Cheng (Ref. 9). His values are slightly lower than ours as his polarizer was only 90% efficient.

[24] H. A. Jahn and E. Teller, Proc. Roy. Soc. (London) **A161**, 220 (1937).

[25] G. D. Watkins, in *Symposium on Radiation Effects in Semiconductor Components* (Journées d'Electronique, Toulouse, France, 1968), p. A1-9.

[26] L. I. Schiff, *Quantum Mechanics* (McGraw-Hill Book Co., New York, 1949), p. 247.

to calculated dichroic ratios which are equal to the experimental ones within the experimental error.

B. Uniaxial Stress Studies

1° Electronic Reorientation

We have measured the dichroism versus applied stress for various infrared beam and stress directions. The results are presented in Fig. 11 and in Table I. In Table I, they are compared with the ones obtained by Cheng.[9] These uniaxial stress studies performed at low temperatures have allowed the determination of the shape of the transition, as has been previously described as well as the exact values of the dichroic ratios of the transition associated to D_i defects (since the background photoconductivity was determined and found to be ~zero). It has been established that the dichroic ratios were comparable for boron- and aluminum-doped samples (Table I).

The values of the dichroic ratios also give information about the reorientation and electronic configuration of the defects since the different electronic configurations of the defect become nonequivalent when applying a stress to the sample; it is this aspect we shall discuss in this section. We give, in the Appendix, a detailed description of the method used to calculate the dichroism for the type of transition described in Sec. IV A. The resulting formulae are contained in Table II. These formulae use the fact that the photoconductive transition we observe corresponds to a volume oscillator. To determine the shape of the ellipsoid of rotation, the distribution of dipole moments was resolved into components along the z axis (γ^2) and in the xy plane (α^2). The ratio α^2/γ^2 determines the value of the dichroism at stress saturation. We give in Table I the experimental values for different infrared and stress directions. They must be compared with the calculated

TABLE II. Dichroic ratio for a dipole moment distribution with a trigonal symmetry.

Stress direction	Infrared direction	$E_\perp/E_\parallel$	Dichoric ratio
[111]	[1$\bar{1}$0]	$\frac{[\bar{1}\bar{1}2]}{[111]}$	$\frac{n_a(\frac{3}{2}\alpha^2)+n_b(\frac{5}{2}\alpha^2+4\gamma^2)}{n_a(3\gamma^2)+n_b(4\alpha^2+\gamma^2)}$
[110]	[001]	$\frac{[1\bar{1}0]}{[110]}$	$\frac{n_a(3\alpha^2)+n_b(\alpha^2+4\gamma^2)}{n_a(\alpha^2+4\gamma^2)+n_b(3\alpha^2)}$
[110]	[1$\bar{1}$0]	$\frac{[001]}{[110]}$	$\frac{n_a(2\alpha^2+2\gamma^2)+n_b(2\alpha^2+2\gamma^2)}{n_a(\alpha^2+4\gamma^2)+n_b(3\alpha^2)}$
[100]	[011]	$\frac{[01\bar{1}]}{[011]}$	1.00
[100]	[010]	$\frac{[001]}{[100]}$	1.00

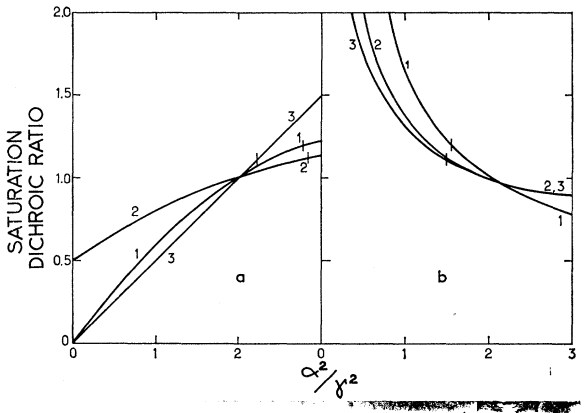

FIG. 12. Theoretical dichroic ratio at stress saturation for different stress and infrared beam directions as a function of α^2/γ^2: (a) $B_2>0$; (b) $B_2<0$. Curves (1)-stress=[110]; IR=[001]; curves (2)-stress=[110]; IR=[1$\bar{1}$0]; curves (3)-stress=[111]; IR=[1$\bar{1}$0]. The vertical lines show the experimental values.

values which are shown in Fig. 12 as a function of α^2/γ^2 for two different hypotheses: (1) the term B_2 of the piezospectroscopic tensor is >0 or (2) B_2 is <0. In the first case ($B_2>0$), the defect responds to the stress in a way which favors the configurations for which the compressional strain is greater along the z axis than in the xy plane (e.g., for a [111] stress direction,configuration a is favored). In the other case ($B_2<0$), these configurations are unfavored. We achieve a much better agreement with our experimental findings by choosing $B_2<0$. This gives the value of α^2/β^2 as ~1.53.

Using this value for α^2/β^2, the magnitude of B_2 can be determined by measuring the dichroic ratios as a function of applied stress. The experimental points are shown in Fig. 10 and are compared with the theoretical curves obtained using a value of B_2 of -12 eV/(unit strain). This value is of the same order of magnitude as has been observed for the stress response of other defects in silicon.[8,9,20,27–31] The measured points fall on the theoretical curves within the experimental error (± 0.02). We believe that this agreement gives a good confirmation of the chosen configuration.

2° Atomic Reorientation

In the proposed configuration, there is only one type of equivalent atomic site. This means that no atomic reorientation is possible with the application of the stress at higher temperatures. We have found no measurable dichroism of the energy levels arising from the D_i defects after stressing the sample at room temperature, cooling it under stress down to 77°K, and

[27] G. D. Watkins and J. W. Corbett, Phys. Rev. **138**, A543 (1965).
[28] G. D. Watkins and J. W. Corbett, Phys. Rev. **121**, 1001 (1961).
[29] G. D. Watkins and J. W. Corbett, Phys. Rev. **134**, A1359 (1964).
[30] E. L. Elkin and G. D. Watkins, Phys. Rev. **174**, 881 (1968).
[31] L. J. Cheng, J. C. Corelli, J. W. Corbett, and G. D. Watkins, Phys. Rev. **152**, 761 (1966).

then removing the stress before the measurement. Cheng[9] has reported the same negative result for similar studies where the stress was applied at 150°C and removed at room temperature. These results do not rule out the possibility that the D_i defects might reorient atomically at another temperature. However, if the annealing at ~300°C occurs by D_i defect motion, the negative results at room temperature and 150°C are probably sufficient to eliminate the possibility of atomic reorientation. On the other hand, if the D_i defects do not move until a higher temperature (as is possible), higher temperatures also might be necessary before atomic reorientation would occur. But the near complete disappearance of the D_i defects at ~300°C makes it extremely unlikely that information could be obtained using stresses at temperatures above 300°C.

C. Charge State—Discussion

From the uniaxial stress experiments we deduce that the symmetry of the D_i defects is C_{3v} and that the photoconductivity transition corresponds to a volume oscillator. We will now discuss the charge state of the defect which is observed. As has been previously pointed out, we can eliminate at once the possibility of a double positive charge state, since we know from Watkins's experiments that the interstitial Al^{++} has a T_d symmetry as opposed to the C_{3v} symmetry of D_i defects.

Since our samples are p-type samples, the possible charge states which are to be expected are a single positive one or a neutral one.

It has been observed in lifetime studies[32] that a neutral defect, that is impurity-dependent, was associated to a level which has approximately the same energy position as the one associated to D_i defect. However, photoconductivity studies performed by Vavilov *et al.*[33] lead them to the conclusion that D_i defect was in a positive charge state.

We will discuss these two possibilities in an approach like the one of Yamaguchi[34] and assuming that the C_{3v} symmetry, which is observed for D_i defect originates from a Jahn-Teller distortion of a T_d configuration. A theoretical treatment of the carbon interstitial in diamond (which has a T_d configuration) has been given by Yamaguchi[34] who uses a linear combination of atomic orbitals-molecular orbital (LCAO-MO) treatment. If we build orbitals for D_i defects in the same manner that was used by Yamaguchi for carbon interstitial, the one-electron orbitals involved transform as a_1 and t_2 in T_d. If we assume that the charge state observed is a neutral charge state the probable three-electron ground state is a $^2T_2$ state in T_d. This state being degenerate, it is possible to get a Jahn-Teller distortion from T_d to C_{3v}. The $^2T_2$ state will be decomposed into ^2E and $^2A_1$ states in C_{3v} symmetry. The ground state of D_i defects would then transform as $^2A_1$ in C_{3v} since the ^2E state is degenerate and would give a further Jahn-Teller distortion. States of these symmetries would result in a volume oscillator transition and, thus, the experimental data are consistent with a neutral charge state.

If we now assume that the charge state is singly positive, the lowest two electron states which can be formed for the D_i defect are probably $^1A_1$ and $^3T_2$ states in T_d symmetry. Since the first one uses only s states of B^+ or Al^+, while the $^3T_2$ state uses s and p states of B^+ or Al^+, and since there are of the order of 5 eV between $1s^22s2p$ and $1s^22s^2$ of the boron ion B^+, it is more likely that the ground state is $^1A_1$. In this case, there will not be a Jahn-Teller distortion of the defect from T_d.

In summary, it is possible to predict a Jahn-Teller distortion from T_d to C_{3v} for a neutral charge state but this is difficult for a positive charge state; thus, the results lean to the interpretation of the D_i defect as being in the neutral charge state. However, this is a highly tentative conclusion and is contradictory to Vavilov's results. It is also somewhat strange, but not impossible because of the possible existence of long-lived nonequilibrium states, that the neutral charge state is observed at 4.2°K, where the Al^{++} is the equilibrium charge state.[2–4] Therefore, although the C_{3v} is fairly well supported by the experimental evidence, the charge state is only tentatively assigned as neutral.

V. SUMMARY

We conclude that the D_i defects which give rise to energy levels located at $E_v+0.395$ eV in aluminum-doped silicon and $E_v+0.430$ eV in boron-doped silicon as measured by infrared photoconductivity are dopant atoms in interstitial positions. The defect production process is probably one where silicon interstitials, formed randomly by the irradiation, migrate to substitutional acceptor atoms and change places with them. The model we deduce is one where the defect distorts out of its original tetrahedral symmetry to a configuration with C_{3v} symmetry. This distortion could be a manifestation of the Jahn-Teller effect. The principal features confirming these conclusions are summarized as follows:

(1) The D_i defects are formed at irradiation temperatures as low as 4.2°K, where only motion of the silicon interstitial is possible.[2–4] Even at irradiation temperatures of 20.4 and 77°K, vacancy motion was found to be small in most cases, and the D_i defects were still formed.

(2) The energy-level position is slightly different in samples with different dopants, showing the presence of the dopant atom in the D_i defect.

(3) The D_i defects anneal, at least in part, at ~250–300°C which is in the same temperature region found

[32] J. A. Naber, H. Horiye, and E. G. Wikner, General Atomic Report No. 8016, p. 68, 1967 (unpublished).
[33] V. S. Vavilov, E. N. Loktova, and A. F. Plotnikov, J. Phys. Chem. Solids **22**, 31 (1961).
[34] T. Yamaguchi, J. Phys. Soc. Japan **18**, 368 (1963).

for the annealing of aluminum interstitials in electron paramagnetic resonance studies.[3,4]

(4) The electronic reorientation was studied by stress-induced alignment at 77°K. The measured dichroisms were in good agreement both in sense and magnitude with the predictions of a model where the transition is from the valence band to a defect state with C_{3v} symmetry for which the dipole moment distribution is an ellipsoid of rotation.

ACKNOWLEDGMENTS

The authors thank Professor P. Baruch, who directed this study, for his interest and valuable discussions and for providing all of the facilities during the course of the experiments. We also thank our colleagues in the semiconductor group at the Université de Paris. In particular, one of us (M.C.), would like to express her appreciation to Dr. J. E. Fischer and Dr. J. Zizine. We are grateful to S. Squelard and C. Picard who provided very competent technical help, as well as to E. d'Artemare and M. Vidal for assistance in performing the irradiations. We thank Dr. B. Goldstein for critical reading of the manuscript and discussion of the results. We also thank Dr. G. D. Watkins for communicating his unpublished results to us.

APPENDIX

Here we shall briefly describe the derivation of the formulas used to calculate the dichroism expected to arise from a transition from a defect state with trigonal symmetry to a carrier band upon the application of uniaxial stress.

With the application of stress to the crystal, the configurations may become nonequivalent in energy. The energy of a defect in a stress field can be written as[35]

$$\epsilon = \mathbf{B}:\mathbf{S}:\mathbf{\Sigma}, \tag{A1}$$

where $\mathbf{\Sigma}$ is the second-rank stress tensor, $\mathbf{S}$ is the fourth-rank elasticity tensor, and $\mathbf{B}$ is the second-rank piezospectroscopic defect-tensor. Kaplyanskii[36] has shown that for a ⟨111⟩ trigonal center, the B matrix has the form

$$\mathbf{B} = \begin{bmatrix} B_1 & B_2 & B_2 \\ B_2 & B_1 & B_2 \\ B_2 & B_2 & B_1 \end{bmatrix} \tag{A2}$$

in the normal cubic system. In our experiment, we do not measure the hydrostatic component of the strain (i.e., the trace of $\mathbf{B}$) and there is only one independent parameter. Viewed physically, this parameter is the relative change in the energy due to the strain along the z axis of the defect compared to that due to the strain in the xy plane. Under stress, the population of the ith defect will reflect the corresponding Boltzmann factor

$$\beta_i = e^{(-\epsilon_i/kT)}. \tag{A3}$$

We can now write down the energy changes and the four populations for the various stress directions as functions of the compressional stress P which is positive in the following formulas.

1. [111] stress:

$$\epsilon_a = -B_1(S_{11}+2S_{12})P - B_2(S_{44})P,$$
$$\epsilon_b = \epsilon_c = \epsilon_d = -B_1(S_{11}+2S_{12})P + B_2(S_{44}/3)P,$$
$$n_a = 4N\beta_a/(\beta_a+3\beta_b), \quad n_b = 4N\beta_b/(\beta_a+3\beta_b).$$

2. [110] stress:

$$\epsilon_a = \epsilon_d = -B_1(S_{11}+2S_{12})P - B_2(S_{44}/2)P,$$
$$\epsilon_b = \epsilon_c = -B_1(S_{11}+2S_{12})P + B_2(S_{44}/2)P,$$
$$n_a = 2N\beta_a/(\beta_a+\beta_b), \quad n_b = 2N\beta_b/(\beta_a+\beta_b).$$

3. [100] stress:

$$\epsilon_a = \epsilon_b = \epsilon_c = \epsilon_d = -B_1(S_{11}+2S_{12})P.$$

All populations are thus equal.

The values of the components of the elasticity tensor that we use are $S_{11} = 7.68\times10^{-13}$, $S_{12} = -2.14\times10^{-13}$, and $S_{44} = 12.56\times10^{-13}$ cm²/dyne.[37]

The dichroic ratio D is given by

$$D = \mathcal{P}_\perp/\mathcal{P}_\parallel = \sum_i n_i \mathfrak{y}_{i\perp}^2 / \sum_i n_i \mathfrak{y}_{i\parallel}^2, \tag{A4}$$

where n_i is the relative population of the ith configuration, and $\mathfrak{y}_{i\perp}$ and $\mathfrak{y}_{i\parallel}$ are the magnitude of the components of the corresponding transition dipole moment $\mathfrak{y}_i$ in the perpendicular and parallel polarization directions, respectively.

In a photoconductivity transition where all orientations of the dipole moment are allowed, the equivalent electric oscillator is a volume oscillator. For a trigonal center, this volume oscillator will be an ellipsoid of rotation about the axis of the center. Then, in the calculation of the dichroic ratio, we will have terms of the form

$$\langle \mathfrak{y}_{ix}^2 \rangle_{\text{av}} = \sum_k (\mathfrak{y}_{ix}^2)_k, \tag{A5}$$

where the summation is over the possible dipole orientations. We shall assume that this sum can be resolved into a component in the xy plane (α^2) and a component along the z direction (γ^2). We give in Table II the expressions for the dichroic ratios as a function of these components α^2 and γ^2 and of the populations n_i. The populations to be used in the formulae are those for the appropriate stress direction.

Of course, these expressions can be used for the case where the transition has either an xy type dipole (then $\gamma^2=0$) or a z-type dipole (then $\alpha^2=0$).

[35] J. F. Nye, *Propriétés Physiques des Cristaux* (Dunod Cie., Paris, 1961).

[36] A. A. Kaplyanskii, Opt. i. Spektroskopiya **16**, 329 (1964) [English transl.: Opt. Spectry (USSR) **16**, 329 (1964)].

[37] H. B. Huntington, in *Solid State Physics*, edited by F. Seitz and D. Turnbull (Academic Press Inc., New York, 1958), p. 274.